Continuum Mech. Thermodyn. (2026) 38:46
https://doi.org/10.1007/s00161-026-01477-1

ORIGINAL ARTICLE

R. Kovács

Interplay of time scales and material nonlinearities in non-Fourier heat conduction

Received: 27 October 2025 / Accepted: 21 April 2026

Abstract The selection of a proper heat conduction model beyond Fourier for complex engineering problems is not straightforward, and the appearance of multiple time scales makes their treatment even more difficult. The present study offers a set of selection criteria for heat equations beyond Fourier. Based on these criteria, it highlights the Guyer-Krumhansl and Jeffreys heat equations as highly viable alternatives due to their flexible continuum thermodynamic background, the ability to inherit results from phonon hydrodynamics, and their applicability to strongly heterogeneous materials such as composite foams. Furthermore, we propose that any heat equation beyond Fourier should be defined by the related linear Onsagerian relations, which clarify the origin of the observable macroscopic transport coefficients. We study the consequences of temperature-dependent thermal conductivity and their relations to the static and dynamic heat conduction time scales, particularly in the case of the Jeffreys heat equation. We also provide numerical demonstrations to support our findings.

1 Introduction

The thermal behavior is usually crucial in the operation of various equipment, especially in the case of heat storage devices [1,2], batteries [3], and structural materials under high thermal loading [4]. The novel and innovative applications often require the use of a heterogeneous material in order to enhance the heat transfer rate and build more efficient devices [5,6]. Typical heterogeneous materials are metal-organic frameworks [7], metal foams [8,9], or layered composites in power electronics with exceptionally high power density.

The complex material structure is, in fact, a multi-component system with multiple time scales, each time scale depending on the corresponding material properties. For instance, a layered composite consists of at least two different materials, and the interface contact resistance influences the heat exchange between the layers. For further discussion, see [10–13]. Furthermore, beyond the material attributes, boundary conditions introduce additional time scales. One glaring example from heat transfer is the definition of Biot number, which prescribes the ratio of two time scales, i.e., comparing heat convection to the characteristic time of heat diffusion. In these situations, it is inevitable to introduce a characteristic length scale as well. In the present study, let us focus on time scales originating from the constitutive relations. Specifically, we investigate how material nonlinearities – such as a temperature-dependent thermal conductivity – immediately influence the

R. Kovács (✉)
Department of Energy Engineering, Faculty of Mechanical Engineering, Budapest University of Technology and Economics, Műegyetem rkp. 3., Budapest H-1111, Hungary
E-mail: kovacs.robert@gpk.bme.hu

R. Kovács
Department of Theoretical Physics, Wigner Research Centre for Physics, Institute for Particle and Nuclear Physics, Budapest, Hungary

Published online: 12 May 2026

heat conduction time scales by dynamically altering propagation speeds and introducing new coupled terms into the evolution equations. However, we must narrow the possibilities of the heat equations we consider here.

Fourier's law is the simplest constitutive relation that satisfies the second law of thermodynamics and possesses well-known properties concerning material nonlinearities (e.g., how to consider a temperature-dependent thermal conductivity [14]). However, it can describe materials and diffusive processes showing only a single time scale heat conduction behavior since only the thermal diffusivity determines the diffusive time scale. This is eligible for situations where any cross-effect disappears, which holds for homogeneous and heterogeneous materials. In the case of homogeneous materials, especially in exceptionally pure crystals [15,16], the phenomenon of second sound (wave propagation) can occur that cannot be modeled with Fourier's law. However, taking a long enough observation period during which the wave effects are negligible, Fourier's law still could be a valid model at the price that fast phenomena will not be resolved. In the case of heterogeneous structures, the presence of different materials can cause deviation from Fourier's law by introducing multiple diffusion mechanisms. Here, the meaning of static and dynamic thermal diffusivity becomes crucial because Fourier's law can provide an acceptable approximation either on short or long time scales [17]. When material nonlinearities are introduced, the static and dynamic time scales do not remain independent, they become coupled depending on the particular state dependencies.

The term "long enough" is indeed difficult to define since it depends on the phenomenon under observation, the material properties, boundary conditions, and the size of the body under observation. Despite such difficulty, this remains a practically valid aspect that can be studied by performing multiple experiments or simulations when a particular problem must be solved. Moreover, depending on the boundary conditions, such a simplified modeling approach is not even meaningful (for instance, in the case of an oscillatory temperature boundary condition). In the present case, however, we focus on the constitutive relations of heat equations with two time scales, which can provide a significantly more detailed description than Fourier's law, e.g., by considering both diffusion and wave propagation. Our aim is threefold. First, we argue about the possible, practically meaningful alternatives to Fourier's law, taking into account various requirements. Second, we study the consequences of temperature-dependent thermal conductivity, exploiting the linear Onsagerian form of the constitutive equations to reveal how material nonlinearities affect the static and dynamic time scales. In parallel, we underline the importance of thermodynamic compatibility, the role of entropy production, and it will highlight the disadvantages of postulates such as those that have occurred in the case of the popular dual-phase-lag (DPL) equation [18–20]. Third, our investigations highlight that in the case of certain heat equations, one might be able to eliminate the resulting nonlinear terms thanks to distinguishing between the static and dynamic time scales by applying proper boundary conditions.

2 Selection criteria for non-Fourier models

Numerous heat equations can be found in the literature, but these models are not systematically utilized. For instance, it is known that the Cattaneo-Vernotte (CV) equation is not applicable for room temperature macroscale bodies [21]. Still, it is often used in various situations such as biological materials because of its hyperbolic (finite propagation speed) attributes [22]. It is impossible to list all misunderstandings; instead, we want to collect specific requirements that can help select the proper heat equation. The mentioned heat equations will be discussed in the following sections.

Hyperbolic or parabolic?

It is often argued that Fourier's heat equation implies an infinite propagation speed due to its parabolic mathematical structure. In fact, this is true, and its Green function is a Gaussian, being non-zero in any time instant at any spatial point [23]. Although this contradicts the physical expectations, parabolic property does not directly limit the applicability of Fourier's law; it is still successfully used in most modern engineering tasks. However, what really limits its use is the number of necessary time scales needed to describe the particular heat conduction problem. This limitation holds for both hyperbolic and parabolic equations. While hyperbolic models are preferable due to their advantageous mathematical properties and the finite speed of propagation, they are not necessarily applicable in general. For example, the CV equation – despite being hyperbolic – is solely applicable in some special situations such as the so-called second sound (damped wave propagation of heat [24,25]).

It is also important to acknowledge the fact that the Guyer–Krumhansl (GK) equation [26] – a parabolic-type model – is successfully utilized to predict the necessary time scale (frequency) of the boundary condition in order to experimentally find second sound in solids, called window condition [27,28]. Therefore, parabolic equations can be valid alternatives to describe wave propagation, and the appearance of wave propagation does not necessarily involve hyperbolic equations. Adding that either hyperbolic or parabolic models are compatible with thermodynamics, such a requirement is inconclusive in the selection process. Furthermore, a hyperbolic extension exists for all parabolic equations and vice versa, particularly apparent – but not exclusive – in the internal variable thermodynamic approach [29,30].

Heat conduction mechanisms – Quantum or continuum?

Three heat conduction mechanisms are considered in the continuum irreversible thermodynamics and phonon hydrodynamics. Namely, these are the diffusive, second sound, and ballistic modes. While the diffusive propagation is well-known since it is the most common phenomenon (and the slowest one), the other two are much more specific (and much faster, too). The second sound is first observed in liquid He, which consists of both superfluid and normal states [31–34]. Since this is a mixture, a two time scale heat conduction model is a viable option. Indeed, the aforementioned CV equation could describe both the slow (diffusive) and the fast (second sound) time scales; however, one must remember that a superfluid is a quantum fluid. Consequently, the CV equation may effectively describe the emergent quantum effects coupled to heat conduction, although it is not an inherently quantum heat conduction model. Moreover, the CV equation's thermal conductivity is not quantized, contrary to the experiments [35], but follows the classical interpretation.

In ballistic heat conduction, the situation is analogous, but this mode shows propagation with the speed of sound [36]. Although phonon hydrodynamics in the framework of rational extended thermodynamics is a suitable approach for both second sound and ballistic propagation with strong predictive possibilities [27], it remains an effective model similar to a continuum irreversible thermodynamic framework. Phonon hydrodynamic equations are derived from the Boltzmann equation, including a simplified collision term through the momentum series expansion, i.e., a mean field is determined only. In that sense, a continuum approach also allows the interpretation that the corresponding field quantity is a mean field in the same sense as a momentum series expansion. On one hand, this propagation mode can be interpreted as a thermo-mechanical effect in which the thermal expansion becomes strong enough at low temperatures (< 20 K) to show an additional wave propagation in the temperature field. On the other hand, observing such fast phenomena experimentally introduces its own complexities, e.g., a bolometer could be used to record the temperature change on the microsecond scale [16]. Consequently, thermal radiation is built into the measurement method, and thus neither the heat conduction phenomenon nor the measurement method itself is free from quantum effects. Overall, when selecting a heat conduction model, one must be aware that these provide only an effective description by increasing the number of state variables (together with their tensorial order), manifesting in the increase of time scales.

Homogeneous or heterogeneous?

The macroscopic observation of second sound and ballistic modes required special materials such as ultra-pure crystals [37,38]. However, most materials used in the engineering practice are heterogeneous, either by porosity or consisting of multiple components. Similarly to the low-temperature phenomena, a multi-component system can result in non-Fourier heat conduction depending on the length and time scales [39,40]. The interaction of the different components introduces parallel heat conduction channels, analogous to different heat conduction mechanisms. Hence, the time evolution of such a body can show a multiple time scale behavior. Such materials, for instance, are composite metal foams, rocks, and metal-organic frameworks.

Furthermore, the phonon hydrodynamic models lose their validity in macroscopic, room temperature situations where the Knudsen number is not necessarily meaningful. For such heterogeneous materials, only a continuum model can be viable. Therefore, it seems reasonable that the following alternative heat conduction model after Fourier should unify certain aspects from phonon hydrodynamics in order to preserve its predictive power, and also consists of at least two diffusive time scales to maintain the ability to model complex material structure on a macroscopic scale.

Postulates or second law?

Postulated models can be easily incompatible with thermodynamics, particularly with the second law. For example, the popular DPL equation cannot be solved in the form as it is postulated [41], and a Taylor series expansion is used to obtain an approximation. This expansion is not convergent, leading to ill-posed problems and stability issues depending on the order of expansion [18–20]. Although the DPL approach resembles a unification regarding the T-representation of various heat equations, and can be helpful in linear situations, we will soon see that it inevitably fails for nonlinear problems due to the missing thermodynamic background.

The situation is similar to the thermomass equations, which treat heat as a fluid with effective mass, since the constitutive equations are not derived using thermodynamics. Moreover, even its basic concept is unclear since the approach mixes the mass and energy balances as an energy-mass equivalence is postulated, assuming the existence of thermons. On the contrary, thermodynamic compatibility ensures the existence of stable equilibrium [42], and reveals functional relationships between the transport coefficients [43]. For example, in the framework of phonon hydrodynamics, it is known that the thermal conductivity and the relaxation time are not independent because the collision frequency of phonons influences both [27]. This functional connection is also present in a continuum approach, and is even more crucial for complex models.

Model selection

In summary, when one must select a heat equation beyond Fourier, numerous aspects emerge, and the selection process is complex due to the fragmentation of the corresponding literature [20].

Based on the criteria mentioned above, two particular heat equations stand out as highly versatile and prime candidates, the GK and the Jeffreys heat equations. While they are not the exclusive options in the broader literature, they prove to be favorable selections within the current framework. The GK equation is outstanding because it can inherit properties from phonon hydrodynamics and continuum thermodynamics, depending on which interpretation and transport coefficients are considered. Moreover, due to the hydrodynamic background of the GK equation, even heat vortices are included. The Jeffreys heat equation, however, is the only heat equation that consists of the static and dynamic thermal conductivity, and this model can only be derived within the internal variable framework. Both models can be reduced to the CV equation; therefore, they have a hyperbolic limit, and they are capable of modeling the second sound. Additionally, these heat equations have a continuum background; thus, they can also model two diffusive time scales, which is crucial for heterogeneous materials. Their strong thermodynamic origin ensures stability and is helpful in modeling material nonlinearities. In this sense, the GK and Jeffreys equations can support each other but are not exchangeable.

Although there are other models with two heat conduction time scales, many of them exhibit much stronger limitations in this specific context than the GK and Jeffreys equations. The 2-temperature (2T) model – doubling Fourier's law – cannot describe wave propagation, and is only helpful when all transport coefficients are known, otherwise, the parameters might not be unique. The DPL model has no strict thermodynamic origin and suffers from mathematical issues. Concerning the Green-Naghdi equations, only type III would be the closest version to the GK equation. Despite their similarities in T-representation, the Green-Naghdi model relies on the fading memory concept, which is not compatible with any other models, and it is not clear how it can be reduced to Fourier's law.

In parallel, we wish to acknowledge here the importance of models with three or even more time scales [44,45]. Still, the experimental and theoretical difficulties and open questions cannot be reliably answered if the simpler models are not well understood. At this point, let us mention an example that will be discussed soon. The GK equation could have a particular nonlinearity, resulting in an apparent thermal conductivity that depends on the temperature and heat flux gradient. It can be negative even without violating the second law of thermodynamics. This theoretical possibility should first be experimentally proved and understood. If any other model with even more time scales shares a similar property, the design of proper experiments and their evaluation becomes significantly more difficult. Consequently, one conclusion of the present paper is that the two time scale models are far from being completely understood, and thus it is not advantageous to move on to more complex models.

Consequently, in the following, we focus on the GK and Jeffreys heat equations and their thermodynamic background, restricting ourselves to rigid isotropic materials. We define these models by their linear Onsagerian equations, and we show how the temperature-dependent thermal conductivity influences the transport coefficients and their relation to the time scales.

3 Continuum thermodynamic properties of the Guyer–Krumhansl equation

In a continuum irreversible thermodynamic framework, the heat equations must be defined on the Onsagerian level, i.e., by providing the corresponding thermodynamic flux-force relation from which the origin of each transport coefficient becomes apparent. However, we must strongly highlight that these Onsagerian relations are not necessarily unique; they depend on the particular modeling approach and the identification of the thermodynamic fluxes and forces. For instance, in the case of linear models, the macroscopically observable transport coefficients are formed by different Onsagerian coefficients (e.g., in one case, the thermal conductivity λ is defined as $\lambda = l/T^2$, and in the other it is $\lambda = 1/(lT^2)$ [20]). Therefore, the range of the coefficients can change, and thus how certain limits can be realized (e.g, the perfect insulator would be $\lambda = 0$, but it requires different limits in these cases). Another notable difference can emerge in treating internal variables, and thus in the model definition [46]. Namely, it influences the definition of thermodynamic state space, the relations between the heat flux and the internal variable, and thus the allowable state dependence of the Onsagerian coefficients. Although these are not decisive for linear models, nonlinear situations can significantly differ. In the present study, we do not aim to investigate these differences. Still, we wish to underline the importance of model definition strongly, particularly in the case of nonlinear heat conduction, and we show these aspects for the GK and Jeffreys equations.

In the case of the GK equation, let us express the time evolution of the heat flux $\mathbf{q}$ by Eq. (1),

$$\mathbf{q} = \mathbf{L}_1^{(2)} \left(-\rho m \partial_t \mathbf{q} + \nabla \frac{1}{T} + \nabla \cdot \mathbf{B} \right), \tag{1}$$

$$\mathbf{B} = \mathbf{L}_2^{(4)} : (\mathbf{q} \otimes \nabla), \tag{2}$$

where $\mathbf{B}$ is a so-called current multiplier or Nyíri-multiplier [47], defined by Eq. (2) as a direct consequence of the second law [48,49], acting as a relaxed state variable [50]. Here, the symbol $\otimes$ denotes the dyadic (or tensorial) product constructing a second-order tensor from two vectors, while the symbol : represents the double dot product. In Eq. (2), it contracts the fourth-order tensor $\mathbf{L}_2^{(4)}$ with the second-order tensor $(\mathbf{q} \otimes \nabla)$ to yield the second-order tensor $\mathbf{B}$. Furthermore, T denotes the temperature, ∇ is the nabla operator, and the coefficients m (scalar), $\mathbf{L}_1^{(2)}$ (second-order tensor), and $\mathbf{L}_2^{(4)}$ form the macroscopically observable transport coefficients of the GK equation. Their positive definiteness must be ensured in order to preserve the concavity properties of the entropy density and the positive entropy production. Eqs. (1)-(2) are the constitutive equations, and can be solved together with the balance of internal energy,

$$\rho \partial_t e + \nabla \cdot \mathbf{q} = 0, \tag{3}$$

where $e = cT$ expresses the internal energy with c denoting the specific heat, and ρ is the mass density.

Equation (1)-(2) are particularly important, taking into account material nonlinearities, and are valid only for constant m. In case when m is not a constant anymore, additional terms and restrictions emerge [20], for simplicity, let us restrict ourselves to a constant m. The other coefficients can depend on the state space $\{e, \mathbf{q}\}$. However, we omit any $\mathbf{q}$-dependent properties since no clear experimental data is known, especially for macroscopic bodies. Here, let us consider the isotropic case where $\mathbf{L}_1^{(2)}$ reduces to a constant $L_1 > 0$, and

$$\mathbf{B} = \frac{L^{\mathrm{s}} - L^{\mathrm{d}}}{3} (\nabla \cdot \mathbf{q}) \, \mathbf{1} + \frac{L^{\mathrm{d}}}{2} (\mathbf{q} \otimes \nabla + \nabla \otimes \mathbf{q}) + \frac{L^{\mathrm{A}}}{2} \epsilon : (\mathbf{q} \times \nabla) \tag{4}$$

in which the scalar coefficients L^{s}, L^{d}, and L^{A} denote the linearly independent symmetric, deviatoric, and antisymmetric parts of the isotropic fourth-order tensor $\mathbf{L}_2^{(4)}$, respectively. Furthermore, ϵ represents the third-order Levi-Civita tensor, and $\times$ denotes the vector cross product. The double dot product contracts ϵ with the vector $(\mathbf{q} \times \nabla)$ resulting in a second-order tensor. That decomposition shows the appearance of heat flux curl, and the fluid interpretation of the GK equation originating from phonon hydrodynamics.

3.1 Linear case - constant transport parameters

The usual form of the GK equation,

$$\tau \partial_t \mathbf{q} + \mathbf{q} = -\lambda \nabla T + \eta_1 \Delta \mathbf{q} + \eta_2 \nabla (\nabla \cdot \mathbf{q}), \tag{5}$$

is valid only for a linear case, and therefore, one cannot simply substitute the thermal conductivity λ with an arbitrary T-dependent function without considering the Onsagerian equations. In a nonlinear case, e.g., when $L_1 = L_1(T)$, solely Eqs. (1)-(2) are useful, otherwise crucial nonlinear contributions might be neglected. This becomes more apparent by the definition of the transport coefficients,

$$\tau = \rho m L_1, \quad \lambda = \frac{L_1}{T^2}, \quad \eta_1 = L_1 \frac{L_2^{\text{dev}} + L_2^{\text{A}}}{2}, \quad \eta_2 = L_1 \frac{2L_2^{\text{sph}} + L_2^{\text{dev}} - 3L_2^{\text{A}}}{6}. \tag{6}$$

There is an equivalent form for Eq. (5) in which the curl of the heat flux appears by exploiting the vector Laplace identity,

$$\Delta \mathbf{q} = \nabla (\nabla \cdot \mathbf{q}) - \nabla \times \nabla \times \mathbf{q}, \tag{7}$$

$$\tau \partial_t \mathbf{q} + \mathbf{q} = -\lambda \nabla T + (\eta_1 + \eta_2) \nabla (\nabla \cdot \mathbf{q}) - \eta_1 \nabla \times \nabla \times \mathbf{q}, \tag{8}$$

therefore, if $\eta_1 = 0$, the effects of heat vorticity can be omitted.

The transport coefficients (6) are linearly independent of each other; however, they still inherit some functional dependencies from the Onsagerian equations. In a phonon hydrodynamic framework, $\eta_2 = 2\eta_1$, and η_1 is identical with the square of the mean free path of phonons [26,27]. It is a modeling choice whether the continuum or the phonon hydrodynamic background is more advantageous. Either way, the relaxation time τ and the thermal conductivity λ are related. It is crucial to note that m is defined at the fundamental Onsagerian level as a constant coefficient. While macroscopic parameters like $\tau(T)$ and $\lambda(T)$ become temperature-dependent due to $L_1(T)$ (as seen in Eq. (6)), one cannot algebraically invert these definitions to force the constant m to become a variable without overwriting the original thermodynamic state space. Furthermore, the continuum background mathematically enables taking $m = 0$ (implying $\tau = 0$, which removes the hyperbolic wave nature but retains non-local parabolic spatial terms), contrary to the limits of phonon hydrodynamics where setting momentum scattering to zero violates the kinetic theory.

In the linear case, it is possible to eliminate one of the field variables; either T or $\mathbf{q}$ can be used as a sole field from which the other can be restored using the balance equation or the constitutive equations. The T-representation, derived by taking the divergence of the constitutive equation (5) and substituting the internal energy balance (3) with a volumetric heat source Q_v yields

$$\tau \partial_{tt} T + \partial_t T = \alpha \Delta T + (\eta_1 + \eta_2) \partial_t \Delta T + \frac{1}{\rho c_v} \left(Q_v + \tau \partial_t Q_v - (\eta_1 + \eta_2) \Delta Q_v \right). \tag{9}$$

This is particularly interesting since it shows how the volumetric heat source Q_v influences the time evolution if it depends on space and time, which is also a characteristic difference compared to the Fourier heat equation. In Eq. (9), $\alpha = \lambda/(\rho c)$ denotes the thermal diffusivity, and Δ is the Laplacian. Furthermore, the two diffusive time scales are even more apparent if we consider $Q_v = 0$, and realize that Eq. (9) consists of the Fourier heat equation together with its time derivative. In this interpretation, α is the static, and $(\eta_1 + \eta_2)/\tau$ is the dynamic thermal diffusivity [46]. However, this can be realized only in the T-representation. If material nonlinearities are present, i.e., either L_1 or L_2 depends on the temperature, the usual definition of thermal diffusivity becomes questionable [14].

Equation (9) influences the definition of initial and boundary conditions, too. Eq. (9) hides the constitutive relations. For a space-dependent initial condition $T_0(t = 0, x)$, it is impossible to tell how the initial time derivative of the temperature or the heat flux is restricted from a physical point of view without using the constitutive equation (5). In regard to the boundary conditions, a space and time-dependent heat flux boundary condition cannot be defined using only the T-representation. Consequently, it is strongly suggested to treat the GK equation as a system of partial differential equations (3) and (5) without eliminating any field variables, even for the linear case.

3.2 Nonlinear case - T-dependent transport parameters

Let us restrict the present study to the state dependence of the Onsagerian coefficients. More appropriately, we consider only temperature dependence instead of the internal energy density for practical reasons, since we leave the specific heat to be constant, and no mechanical couplings are considered. From a practical point of view, the temperature is measurable, in contrast to the internal energy, internal variable, and heat flux. We acknowledge that although this analysis remains a simplified special case of a more general situation, it

has strict limitations, but opens the discussion towards future experiments and practical aspects that can be discovered in later research.

To take into account the functional dependence between the coefficients, and keeping in mind that additional nonlinear terms might emerge, the Onsagerian equations should be the starting point, exploiting that the material is isotropic,

$$\mathbf{q} = L_1 \left(-\rho m \partial_t \mathbf{q} + \nabla \frac{1}{T} + \nabla \cdot \mathbf{B} \right), \tag{10}$$

$$\mathbf{B} = \frac{L^{\mathrm{s}} - L^{\mathrm{d}}}{3} (\nabla \cdot \mathbf{q}) \, \mathbf{1} + \frac{L^{\mathrm{d}}}{2} (\mathbf{q} \otimes \nabla + \nabla \otimes \mathbf{q}) + \frac{L^{\mathrm{A}}}{2} \epsilon : (\mathbf{q} \times \nabla) \, . \tag{11}$$

We emphasize that Eqs. (10) and (11) constitute strictly linear Onsagerian flux-force relations. Although one might also consider nonlinear Onsagerian relations, such an approach is mathematically and physically distinct from the state-dependence investigated in this study, where the nonlinearity arises exclusively because the transport coefficients depend on state variables. The isotropic decomposition might restrict the physically sound state dependence of the coefficients in Eq. (11), unfortunately, up to now, there is no experimental knowledge on what T-dependence would be meaningful. Therefore, let us simplify the discussion by assuming a one-dimensional situation in which the constitutive equations simplify to

$$q = L_1 \left(-\rho m \partial_t q + \partial_x \frac{1}{T} + \partial_x B \right), \tag{12}$$

$$B = L_2 \partial_x q, \tag{13}$$

thus

$$\rho m L_1 \partial_t q + q = -\frac{L_1}{T^2} \partial_x T + L_1 \partial_x \Big(L_2 \partial_x q \Big) \tag{14}$$

In other words, if $L_1 = L_1(T)$, then a particular T-dependence of the thermal conductivity also appears in all other coefficients. This property is entirely different from Fourier's law, and remains valid for the CV equation in which $L_2 = 0$. Physically, L_1 drives the primary diffusive transport (determining the standard thermal conductivity), while L_2 governs the non-local spatial interactions of the heat flux (related to the mean free path or heat vorticity). If the resulting T-dependence of the relaxation time $\tau(T) = \rho m L_1(T)$ is not satisfactory because of a disagreement with experimental data, one cannot simply mathematically rearrange the definition to force the constant m to be temperature-dependent. As mentioned earlier, m is defined as a constant at the Onsagerian level. To introduce a T-dependent m, the entire thermodynamic derivation must be repeated from the beginning for $m = m(T)$, which would introduce additional nonlinear terms in the constitutive equations. The other way is to propose $\rho = \rho(T)$; therefore, it might be necessary to include mechanical couplings as well, for which one might need to repeat the derivation, depending on the particular problem. These options are discussed in more detail in [20].

There is also an interesting behavior, characteristic only for the GK equation, namely, if $L_2 = L_2(T)$. It yields

$$\partial_x \Big(L_2(T) \partial_x q \Big) = \frac{\mathrm{d}L_2(T)}{\mathrm{d}T} \partial_x T \, \partial_x q + L_2(T) \partial_{xx} q, \tag{15}$$

from which the first one (on the right hand side) can modify the thermal conductivity,

$$\rho m L_1 \partial_t q + q = -\left(\frac{L_1}{T^2} - \frac{\mathrm{d}L_2(T)}{\mathrm{d}T} \partial_x q \right) \partial_x T + L_1 L_2(T) \partial_{xx} q, \tag{16}$$

that is, the apparent thermal conductivity $\hat{\lambda}$ is

$$\hat{\lambda} = \frac{L_1}{T^2} - \frac{\mathrm{d}L_2(T)}{\mathrm{d}T} \partial_x q. \tag{17}$$

This is indeed remarkable since the T-dependent nonlocal term introduces a nonlinear contribution proportional to the temperature gradient; additionally, the heat flux gradient also appears. Since it is impossible to measure the heat flux field point by point practically, thus its gradient cannot be reliably evaluated, however,

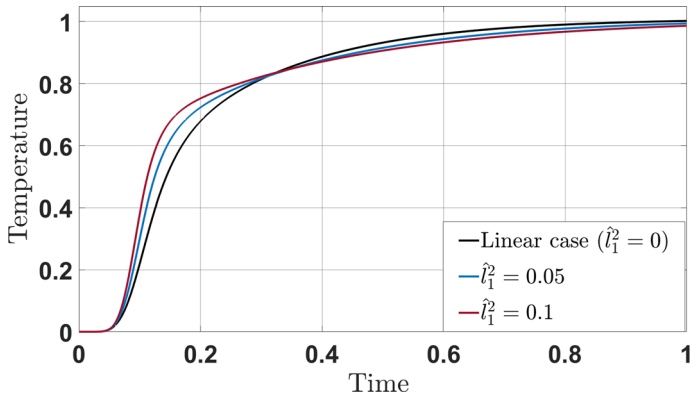

Fig. 1 The rear side (dimensionless) temperature history corresponding to the heat pulse experiment. Three situations are compared: one linear and two nonlinear solutions. The assumed nonlinearity increases the dynamic thermal diffusivity; therefore, the rise in temperature becomes steeper on a short time scale

such material nonlinearity can result in a negative apparent thermal conductivity. It does not influence the presence of two diffusive time scales, but detunes them depending on $L_2(T)$. For instance, if $L_2(T)$ monotonously increases in T, it yields lower apparent thermal conductivity but increases its contribution to the apparent dynamic thermal diffusivity; consequently, the two diffusive time scales become even more separate. Let us note that it still depends on the boundary conditions and the heat flux gradient.

3.3 Numerical demonstration

It is not straightforward how the nonlinear contribution in Eq. (17) changes the apparent thermal conductivity; thus, a brief numerical demonstration is given here. Although it strongly depends on the particular situation – especially on the boundary condition – the numerical simulation of a heat pulse experiment can be insightful. This is a standard method to determine the (apparent) thermal diffusivity. Although minor temperature disturbances are usually applied in that type of experiment, linear models are generally considered, but we aim to exploit the heat flux dependence in Eq. (17).

Using a staggered grid, let us employ an explicit discretization based on [51]. It enables us to solve the nonlinear system of equations without the need to eliminate either q or T; moreover, the q-boundary conditions can be explicitly given without introducing any incompatibilities with the temperature field T. Further details can be found in Appendix A.

Figure 1 shows the typical changes in the rear side temperature history. The two heat conduction time scales remain apparent, there is a quick temperature rise at the beginning and a slower relaxation towards the equilibrium value. This is called over-diffusive propagation, which is typical for heterogeneous materials. This specific nonlinearity is just assumed, has no experimental evidence, but it is applied to test the theoretical concept and whether Eq. (17) is capable of yielding negative apparent thermal conductivity. The specific numerical values chosen for the nonlinearity parameters (e.g., $\hat{l}_1^2 = 0.05$ and 0.1 in the dimensionless framework) were selected purely as order-of-magnitude theoretical demonstrations to show that the mathematical framework is stable and does not violate the second law. Figure 2 shows a 3D plot of Eq. (17) for all space and time points (since q is a field). More appropriately, the apparent thermal conductivity is rescaled using the reference value related to the initial state. It means that right after the heat pulse is applied to the front surface, there is a remarkable chance that such a negative apparent thermal conductivity can be observed. However, the effect is probably hidden on the rear surface, i.e., where the measurement can be performed with the lowest uncertainty.

This short numerical demonstration justifies that a usual experimental setting can result in a negative apparent thermal conductivity without implementing numerous artificial assumptions beyond the particular T-dependence of the nonlocal term. This nonlinearity does not modify the existence and observation of two conduction time scales but influences their ratio.

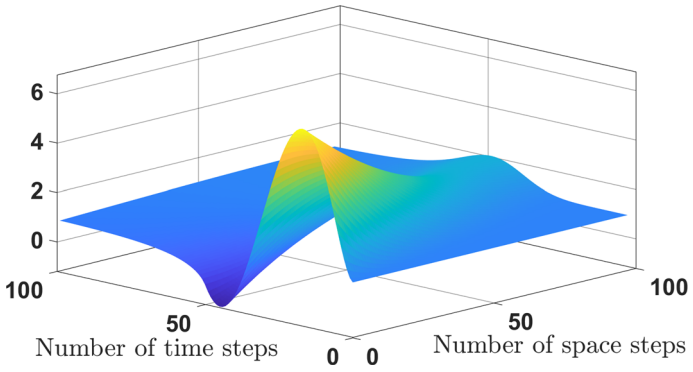

Fig. 2 The ratio of the (static) thermal conductivity and the state-dependent one, demonstrating that the assumed set of parameters and boundary conditions (also used for Fig. 1) yield a negative apparent thermal conductivity. The nonlinear contribution in the apparent thermal conductivity disappears together with the transients

4 Continuum thermodynamic properties of the Jeffreys equation

This particular heat equation can only be derived within the framework of internal variables [52]; therefore, this model is valid only in a continuum interpretation, and it has no phonon hydrodynamic origin. Despite its lack of the capability to unify various approaches as the GK equation does, this is the only model among all heat equations in which there is a separate thermal conductivity for the static and dynamic time scales.

The linear Onsagerian equations are

$$\mathbf{q} = l_{11}\nabla\frac{1}{T} + l_{12}(-m\boldsymbol{\xi}), \tag{18}$$

$$\partial_t\boldsymbol{\xi} = l_{21}\nabla\frac{1}{T} + l_{22}(-m\boldsymbol{\xi}), \tag{19}$$

where $\boldsymbol{\xi}$ is a so-called vectorial internal variable. Within the internal variable framework, $\boldsymbol{\xi}$ acts as an independent state variable defined in the generalized Gibbs relation. However, the second law of thermodynamics strictly governs its time evolution through these Onsagerian relations by introducing cross-couplings and restricting the coefficients to guarantee a positive entropy production. The coefficients must satisfy the inequalities,

$$m \geq 0, \quad l_{11} \geq 0, \quad l_{22} \geq 0, \quad l_{11}l_{22} - l_{12}l_{21} \geq 0 \tag{20}$$

in order to achieve a positive entropy production. These form the macroscopically observable transport parameters in the constitutive equation, analogously to the GK equation.

4.1 Linear case - constant transport parameters

In the linear case, it is straightforward to eliminate the internal variable $\boldsymbol{\xi}$, resulting in the Jeffreys equation,

$$\tau\partial_t\mathbf{q} + \mathbf{q} = \tilde{\lambda}_1\nabla\frac{1}{T} + \tilde{\lambda}_2\partial_t\nabla\frac{1}{T}, \tag{21}$$

where the coefficients are defined by

$$\tau = \frac{1}{l_{22}m}, \quad \tilde{\lambda}_1 = \frac{\det l_{ij}}{l_{22}}, \quad \tilde{\lambda}_2 = l_{11}\tau, \tag{22}$$

relations, in which $\tilde{\lambda}_1$ and $\tilde{\lambda}_2$ are the static and dynamic thermal conductivity, respectively. It is straightforward to realize that Eq. (22) shares certain properties with the coefficients of the GK equation. First, all transport parameters are in relation to the (static) thermal conductivity $\tilde{\lambda}_1$. Second, both can be reduced to the CV equation, where $l_{11} = 0$ is necessary. However, if $m = 0$ (it must be taken into account on the Onsagerian

level (18)-(19)), the Jeffreys equation reduces to Fourier's law as it decouples the heat flux from the internal variable.

Usually, the resulting T^2 from the derivative of $1/T$ is omitted in a sense that is built into the definition of thermal conductivity. This is not an issue with the static (Fourier) part, but it is not straightforward in the mixed derivative term. It is possible to treat T^2 as a reference temperature, such as T_0^2; thus, it is a constant in this sense, and the additional nonlinear terms can be avoided. If this is not the case, then $2\lambda_2 T^{-3}\partial_t T\nabla T$ term will appear on the r.h.s. of Eq. (21).

The T-representation of Eq. (21) formally resembles to the GK equation in the linear regime, thus

$$\tau\partial_{tt}T + \partial_t T = \hat{\alpha}_1\Delta T + \hat{\alpha}_2\partial_t\Delta T + \frac{Q_v}{\rho c_v} + \frac{\tau}{\rho c_v}\partial_t Q_v, \tag{23}$$

wherein $\hat{\alpha}_{1,2}$ are the corresponding static and dynamic thermal diffusivity. The Jeffreys equation, more properly, its T-representation can be T-equivalent with the GK equation if the heat source is not space-dependent, $Q_v = Q_v(t)$, and the curl of the heat flux is omitted in the GK model ($\eta_1 = 0$). They can describe the same temperature history even in a three-dimensional situation. It feels important to highlight that this equivalence is only valid for the temperature field because these models retain different constitutive relations. Furthermore, thanks to the T-equivalence, the static and dynamic thermal diffusivity parameters can be equal, however, the Jeffreys equation provides a deeper insight by characterizing the given body with its static and dynamic thermal conductivity. This remarkable property can be exploited in nonlinear situations.

4.2 Nonlinear case - T-dependent transport parameters

The Jeffreys equation is peculiar in the sense that there are multiple possibilities to have a T-dependent (static) thermal conductivity since all four Onsagerian transport coefficients are present in the definition of $\tilde{\lambda}_1$. It is important to highlight that eliminating the internal variable $\boldsymbol{\xi}$ is necessary, since it is an unknown field and one cannot prescribe either initial or boundary conditions. Eliminating $\boldsymbol{\xi}$ yields:

$$-\partial_t\left[\frac{1}{l_{12}m}\left(\mathbf{q} - l_{11}\nabla\frac{1}{T}\right)\right] = l_{21}\nabla\frac{1}{T} + \frac{l_{22}}{l_{12}}\left(\mathbf{q} - l_{11}\nabla\frac{1}{T}\right), \tag{24}$$

in which it becomes apparent that l_{11} and l_{21} can introduce further nonlinear contributions into the evolution equation (and m is still considered to be a constant).

Type I: $l_{11} = l_{11}(T)$

In that case, the static and dynamic thermal conductivity become T-dependent,

$$\tau\partial_t\mathbf{q} + \mathbf{q} = \left(l_{11}(T) - \frac{l_{21}l_{12}}{l_{22}}\right)\nabla\frac{1}{T} + \tau l_{11}(T)\partial_t\nabla\frac{1}{T} + \tau\frac{\mathrm{d}l_{11}(T)}{\mathrm{d}T}\partial_t T\nabla\frac{1}{T}, \tag{25}$$

where

$$\tilde{\lambda}_1(T) = l_{11}(T) - \frac{l_{21}l_{12}}{l_{22}}, \quad \tilde{\lambda}_2(T) = \tau l_{11}(T). \tag{26}$$

It means that the same temperature dependence drives both time scales while $\tau = 1/(l_{22}m)$ remains constant.

Type II: $l_{12} = l_{12}(T)$

The resulting constitutive equation reads

$$\tau\partial_t\mathbf{q} + \mathbf{q} = \tilde{\lambda}_1(T)\nabla\frac{1}{T} + \tilde{\lambda}_2\partial_t\nabla\frac{1}{T} + \tau\frac{1}{l_{12}(T)}\frac{\mathrm{d}l_{12}(T)}{\mathrm{d}T}\partial_t T\left(\mathbf{q} - \frac{\tilde{\lambda}_2}{\tau}\nabla\frac{1}{T}\right), \tag{27}$$

in which it is remarkable to investigate the last nonlinear term. Here, eventually, one can realize Fourier's law with the dynamic thermal conductivity, which can be an acceptable approximation of the Jeffreys equation

for fast phenomena. That is, if the boundary conditions dictate a fast heat transfer, the linear Jeffreys equation reads

$$\tau \partial_t \mathbf{q} = \tilde{\lambda}_2 \partial_t \nabla \frac{1}{T}. \tag{28}$$

Suppose one omits any mathematically delicate possibilities concerning the smoothness of these fields (e.g., jumps, point-like heat sources, etc.). In that case, Eq. (28) can be reduced to Fourier's law including the dynamic thermal conductivity. In other words, Eq. (27), despite its complicated nonlinear structure, can be simplified to the dynamic Fourier's law when the dynamic time scale dominates the heat conduction process. Additionally, it must be noted that this approximation is only valid if the existing two conduction time scales are indeed notably different – that is, when the ratio of the dynamic time scale to the static time scale is sufficiently large,

$$\frac{\tilde{\lambda}_2}{\tau \tilde{\lambda}_1} \gg 1. \tag{29}$$

Type III: $l_{21} = l_{21}(T)$

This is the most straightforward situation since $l_{21}(T)$ does not influence the other transport parameters, and therefore only the static thermal conductivity depends on the temperature without any additional nonlinear contributions,

$$\tau \partial_t \mathbf{q} + \mathbf{q} = \tilde{\lambda}_1(T) \nabla \frac{1}{T} + \tilde{\lambda}_2 \partial_t \nabla \frac{1}{T}. \tag{30}$$

Type IV: $l_{22} = l_{22}(T)$

This option makes all transport coefficients to be T-dependent without further nonlinear contributions, and

$$\tau(T) \partial_t \mathbf{q} + \mathbf{q} = \tilde{\lambda}_1(T) \nabla \frac{1}{T} + \tilde{\lambda}_2(T) \partial_t \nabla \frac{1}{T}, \tag{31}$$

in which both time scales are driven again by the same temperature dependence. However, this situation is different from the previous one (Type I), because $\tilde{\lambda}_2/\tau = l_{11}\tau/\tau = l_{11}$, which is a constant. Consequently, the dynamic scale can remain constant while the other one can either be closer or farther, depending on $\mathrm{d}l_{22}/\mathrm{d}T$. Furthermore, by applying the dynamic Fourier equation again (28), one could assume that

$$\tau(T) \partial_t \mathbf{q} = \tilde{\lambda}_2(T) \partial_t \nabla \frac{1}{T} \quad \Rightarrow \quad \partial_t \mathbf{q} = \frac{l_{11}\tau(T)}{\tau(T)} \partial_t \nabla \frac{1}{T} \quad \Rightarrow \quad \mathbf{q} = l_{11} \nabla \frac{1}{T}. \tag{32}$$

Although the possibility of eliminating a nonlinearity and obtaining an acceptable approximation utilizing Fourier's law is indeed attractive, there is no experimental evidence up to now for confirmation. Additionally, the validity of this approximation depends heavily on the boundary conditions and is valid only for homogeneous initial conditions. For inhomogeneous initial states, the given nonlinearity strictly dictates the physically compatible initial states, and thus it cannot be eliminated.

4.3 Numerical demonstration

Our goal here is to numerically validate the theoretical prediction that the type II nonlinearity can be effectively eliminated using the dynamic time scale. To simulate a scenario where the dynamic time scale dominates, we utilize a time-scale ratio of 10, which represents a physically realistic setup for a strongly heterogeneous material such as a layered composite (detailed in Appendix B) . Similarly to the GK equation, we rescale the corresponding equations again and apply the staggered field discretization method [51]. In contrast to the GK equation, here we utilize a temperature boundary condition that is periodic in time to represent fast phenomena better.

Figure 3 shows the prescribed boundary condition on the front side, and the resulting temperature history on the rear side following the linear Jeffreys equation compared to the dynamic Fourier equation. It is visible that the dynamic Fourier equation can follow the phase and provides an acceptable approximation to the

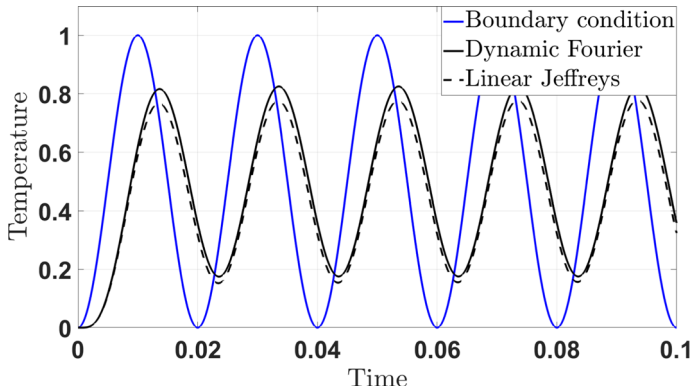

Fig. 3 The front side (dimensionless) temperature boundary condition is compared to the rear side temperature history, demonstrating that the dynamic Fourier equation indeed approximates well the (linear) Jeffreys heat equation for a fast heat conduction process

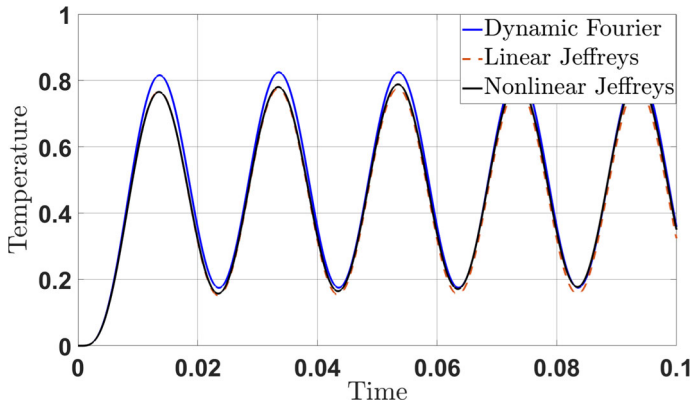

Fig. 4 The rear side (dimensionless) temperature history, comparing the solution of the Jeffreys equation with type II nonlinearity to its linear version and the dynamic Fourier equation using the temperature boundary condition depicted in Fig. 3

temperature amplitude of the linear Jeffreys model. Crucially, Figure 4 demonstrates the solution of the type II nonlinear Jeffreys equation, which, for the dynamic scale, is almost indistinguishable from the linear Jeffreys equation and falls close to the dynamic Fourier equation. This provides strong computational proof for our theoretical claim, under fast boundary conditions, the complex material nonlinearity is physically suppressed, allowing the system to be approximated by the much simpler Fourier equation using the dynamic thermal conductivity.

5 Summary and discussion

In the present study, we have discussed the selection criteria of the heat equation beyond Fourier. We have provided detailed reasoning on the GK and Jeffreys equations, explaining why these heat conduction models could be viable alternatives to the Fourier heat equations. First, continuum models are flexible in the sense of material nonlinearities, experiments, and thus in the modeling capabilities. Second, the GK equation can partially unify the phonon hydrodynamic aspects by inheriting the transport coefficients and their interpretation; however, the continuum background also enables the efficient and effective modeling of heterogeneous materials. Furthermore, the Jeffreys heat equation is peculiar when the thermal conductivity must be temperature-dependent. Uniquely, the Jeffreys equation distinguishes a static and dynamic time scale on the constitutive level, allowing for the elimination of particular effects of material nonlinearities. Third, these models are compatible with the second law of thermodynamics, revealing crucial relationships between the macroscopic transport parameters.

A primary novel contribution of this work is the rigorous demonstration of how material nonlinearities inherently dictate and detune the static and dynamic heat conduction time scales. While existing literature often

under-emphasizes the role of thermodynamics in handling nonlinearities (see, e.g., the postulated DPL equation), we have shown mathematically that state-dependent transport parameters directly couple these scales. Furthermore, we provided a novel systematic breakdown of the nonlinear Jeffreys equation into four distinct types, revealing the exact conditions under which complex nonlinearities can be eliminated and approximated by a dynamic Fourier equation when boundary conditions dictate a fast heat transfer.

Additionally, we have discussed in detail the consequences of the temperature-dependent parameters. In the case of the GK equation, our theoretical framework yields a highly counter-intuitive but thermodynamically consistent novel result. Namely, we have revealed and numerically proved that it is indeed possible to observe a negative apparent thermal conductivity during the transient phase of a standard heat pulse experiment, purely driven by the heat flux gradient even under usual circumstances. Regarding the Jeffreys equation, we have provided four possibilities for taking into account the effects of the temperature-dependent thermal conductivity. Among these options, type III is the most straightforward way to do it, as it will not result in any additional nonlinear contributions and will not affect any other transport parameters. Even further, nonlinear effects in type II and IV might be eliminated when the dynamic time scale dominates the heat conduction process; however, it is conditional, and depends on the boundary conditions, and requires homogeneous initial conditions. For inhomogeneous initial states, evaluating the constitutive equation is necessary to have a physically admissible solution; therefore, one must consider all nonlinear terms. These consequences could not be realized without the thermodynamic background, and it also excludes certain heat equations, such as the popular DPL model, which can also suffer from mathematical issues.

Finally, we highlight that these observations are only theoretical. Up to now, no experimental results are available to avoid artificial assumptions on the T-dependence. For instance, in the Jeffreys equation, we have only considered a special situation in which only one Onsagerian coefficient depends on the temperature. There could be further requirements in practice, and these results must be experimentally confirmed. Despite these current limitations, the provided formulae show how to design experimental settings in the future to separate specific time scales and effects from each other, and the experiments will also be decisive about the viable alternatives of the Fourier equation.

Acknowledgements The research reported in this paper is part of project no. TKP-6-6/PALY-2021, implemented with the support provided by the Ministry of Culture and Innovation of Hungary from the National Research, Development and Innovation Fund, financed under the TKP2021-NVA funding scheme. The research carried out at BME has been also supported by the grant National Research, Development and Innovation Office-NKFIH STARTING24 149487 and by the Sustainable Development and Technologies National Programme of the Hungarian Academy of Sciences (FFT NP FTA). This paper was supported by the János Bolyai Research Scholarship of the Hungarian Academy of Sciences, Hungary.

Funding Open access funding provided by Budapest University of Technology and Economics.

Author contribution R.K. is the sole author of the present manuscript and therefore responsible for the research, writing, and revision.

Data Availibility No datasets were generated or analysed during the current study.

Declarations

Competing interests The authors declare no competing interests.

Appendix A

Let us first gather the one-dimensional equations we solve numerically for which we need the balance equation of internal energy,

$$\rho c \partial_t T + \nabla \cdot q = 0, \tag{33}$$

and the constitutive equation,

$$\tau \partial_t q + q = -\hat{\lambda}(T, q)\partial_x T + l^2(T)\partial_{xx} q, \tag{34}$$

hence we have an evolution equation for both fields. For a heat pulse experiment, the initial condition describes a homogeneous equilibrium, i.e., $T(x, t = 0) = T_0$, in which state the heat flux field and also their time derivatives are zero. For numerical reasons, it is advantageous to prescribe a smooth function on the boundary. Here, we apply $q(x = 0, t) = q_{\max}(1 - \cos(2\pi t/t_p))$, where t_p is the length of the heat pulse. Let us consider a perfectly insulated rear side, i.e., $q(x = L, t) = 0$ for simplicity, as it does not modify our observations about the apparent thermal conductivity.
Furthermore, let us utilize dimensionless quantities for which the characteristic length scale is chosen to be the sample thickness L, and the time scale is L^2/α, i.e., we use the Fourier number as the dimensionless time. The temperature is rescaled using the difference between the adiabatic equilibrium temperature (T_{end} and the initial temperature T_0, that is,

$$\hat{T} = \frac{T - T_0}{T_{\text{end}} - T_0}, \tag{35}$$

therefore the temperature is scaled between 0 and 1. These will result in the following dimensionless set of equations (using the hat notation),

$$\hat{\tau}_{p,0}\partial_{\hat{t}}\hat{T} + \partial_{\hat{x}}\hat{q} = 0, \tag{36}$$

$$\hat{\tau}\partial_{\hat{t}}\hat{q} + \hat{q} = -\hat{\tau}_p(\hat{T}, \hat{q})\partial_{\hat{x}}\hat{T} + \hat{l}^2(\hat{T})\partial_{\hat{x}\hat{x}}\hat{q}, \tag{37}$$

where $\tau_{p,0} = \alpha t_p/L^2$, and let us consider the simplest nonlinearity in $\hat{l}^2$, i.e., $\hat{l}^2 = \hat{l}_0^2 + \hat{l}_1^2\hat{T}$, and $\hat{l}_0^2 = l_0^2/L^2$. The reference value $\hat{l}_0^2$ is related to the initial temperature, and as the heat pulse experiment always heats the sample, that nonlinearity cannot result in negative $\hat{l}^2$, and thus the second law of thermodynamics is not violated. Furthermore, $\hat{\tau}_p(\hat{T}, \hat{q}) = \tau_{p,0} + \hat{l}_1^2\partial_{\hat{x}}\hat{q}$. The specific numerical values chosen for the demonstration in Section 3 (e.g., $\hat{l}_1^2 = 0.05$ and 0.1) were selected as physically plausible, order-of-magnitude perturbations to distinctly visualize the over-diffusive transient behavior without violating the positive definiteness required by the second law. Furthermore, the applied linear T-dependence is also only for demonstrative reasons, no particular physical mechanisms is assumed.
These equations were solved with an explicit discretization,

$$\hat{\tau}_{p,0}\frac{\hat{T}_j^{n+1} - \hat{T}_j^n}{\Delta\hat{t}} + \frac{\hat{q}_{j+1}^n - \hat{q}_j^n}{\Delta\hat{x}} = 0, \tag{38}$$

$$\hat{\tau}\frac{\hat{q}_j^{n+1} - \hat{q}_j^n}{\Delta\hat{t}} + \hat{q}_j^n = -\left(\hat{\tau}_{p,0} - \hat{l}_1^2\frac{\hat{q}_{j+1}^n + \hat{q}_{j-1}^n}{2}\right)\frac{\hat{T}_j^n - \hat{T}_{j-1}^n}{\Delta\hat{x}} + \hat{l}^2(\hat{T}_j^n)\frac{\hat{q}_{j+1}^n - 2\hat{q}_j^n + \hat{q}_{j-1}^n}{\Delta\hat{x}^2}, \tag{39}$$

where the indices n and j denote the time and space coordinates, respectively, and Δt, Δx express the corresponding time and space steps. We do not intend to thoroughly investigate the numerical properties of the difference equations, but we have paid attention to the stability and convergence by testing for multiple time and space steps.

Appendix B

Let us summarize first the one-dimensional equations we solve, the balance equation for the internal energy,

$$\rho c \partial_t T + \partial_x q = 0, \tag{40}$$

and the constitutive equation related to type II nonlinearity,

$$\tau \partial_t q + q = \tilde{\lambda}_1(T)\partial_x\frac{1}{T} + \tilde{\lambda}_2\partial_t\partial_x\frac{1}{T} + \tau\frac{1}{l_{12}(T)}\frac{\mathrm{d}l_{12}(T)}{\mathrm{d}T}\partial_t T\left(q - \frac{\tilde{\lambda}_2}{\tau}\partial_x\frac{1}{T}\right), \tag{41}$$

for which we prove that the dynamic time scale can effectively eliminate the additional nonlinear contribution, and the linear (dynamic) Fourier equation can approximate its solution. In order to have a better representation of fast phenomena, let us apply a temperature boundary condition that is periodic in time, i.e., $T(x=0,t) = T_0(1-\cos(\pi t/t_p))$, and let the rear side be adiabatic. Therefore, one can directly adjust the desired frequency, hence the appearing time scale on the boundary. Furthermore, we set the ratio of the dynamic and static time scale to 10. This represents a physically viable set of parameters for a strongly heterogeneous material, such as a layered composite capacitor sample in which aluminum and paper layers follow each other successively. The initial condition is a homogeneous equilibrium.

For numerical reasons, we apply again dimensionless quantities, using the same set of characteristic scales as described in Appendix A. The resulting set of dimensionless equations are

$$\hat{\tau}_{p,0}\partial_{\hat{t}}\hat{T} + \partial_{\hat{x}}\hat{q} = 0, \tag{42}$$

$$\hat{\tau}\,\partial_{\hat{t}}\hat{q} + \hat{q} = \hat{\tau}_p(\hat{T})\partial_{\hat{x}}\hat{T} + \hat{\tau}_{p,2}\partial_{\hat{t}}\partial_{\hat{x}}\hat{T} + \hat{\tau}\,\frac{1}{\hat{l}_{12}(\hat{T})}\frac{\mathrm{d}\hat{l}_{12}(\hat{T})}{\mathrm{d}\hat{T}}\partial_{\hat{t}}\hat{T}\left(\hat{q} - \frac{\tilde{\lambda}_2}{\hat{\tau}}\partial_{\hat{x}}\hat{T}\right). \tag{43}$$

These equations are explicitly discretized according to the same method using staggered grids [51], preserving the advantages of the implementation of boundary conditions. The assumed nonlinearity is linear in T, that is, let $l_{12}(T) = l_{12,0} + l_{12,1}\hat{T}$, which reads $\hat{\tau}_p(T) = \hat{\tau}_{p,0} + \hat{\tau}_{p,1}\hat{T}$ in the dimensionless case. The difference equations are

$$\hat{\tau}_{p,0}\frac{\hat{T}_j^{n+1} - \hat{T}_j^n}{\Delta\hat{t}} + \frac{\hat{q}_{j+1}^n - \hat{q}_j^n}{\Delta\hat{x}} = 0, \tag{44}$$

$$\hat{\tau}\frac{\hat{q}_j^{n+1} - \hat{q}_j^n}{\Delta\hat{t}} + \hat{q}_j^n = -\left(\hat{\tau}_{p,0} + \hat{\tau}_{p,1}\hat{T}_j^n\right)\frac{\hat{T}_j^n - \hat{T}_{j-1}^n}{\Delta\hat{x}} + \hat{\tau}_{p,2}\left[\frac{\hat{T}_j - \hat{T}_{j-1}}{\Delta\hat{x}}\right]\Bigg|_n^{n+1} + \hat{\tau}\,\frac{1}{\hat{\tau}_p(\hat{T}_j^n)}\hat{\tau}_{p,1}\frac{\hat{T}_j^{n+1} - \hat{T}_j^n}{\Delta\hat{t}}\left(\hat{q}_j^n - \frac{\tau_{p,2}}{\hat{\tau}}\frac{\hat{T}_j^n - \hat{T}_{j-1}^n}{\Delta\hat{x}}\right), \tag{45}$$

where the $|_n^{n+1}$ notation means that the same difference should be evaluated in these time steps. We do not intend to thoroughly investigate the numerical properties of the difference equations, but we have paid attention to the stability and convergence by testing for multiple time and space steps.

References

1. Feczkó, T., Trif, L., Horák, D.: Latent heat storage by silica-coated polymer beads containing organic phase change materials. Sol. Energy **132**, 405–414 (2016)
2. Németh, B., Németh, Á.S., Ujhidy, A., Tóth, J., Trif, L., Gyenis, J., Feczkó, T.: Fully bio-originated latent heat storing calcium alginate microcapsules with high coconut oil loading. Sol. Energy **170**, 314–322 (2018)
3. Wu, W., Wang, S., Wu, W., Chen, K., Hong, S., Lai, Y.: A critical review of battery thermal performance and liquid based battery thermal management. Energy Convers. Manage. **182**, 262–281 (2019)
4. Formalev, V.F., Kolesnik, S.A., Kuznetsova, E.L., Rabinskii, L.N.: Heat and mass transfer in thermal protection composite materials upon high temperature loading. High Temp. **54**, 390–396 (2016)
5. Han, X.-H., Wang, Q., Park, Y.-G., T'Joen, C., Sommers, A., Jacobi, A.: A review of metal foam and metal matrix composites for heat exchangers and heat sinks. Heat Transfer Eng. **33**(12), 991–1009 (2012)
6. Boomsma, K., Poulikakos, D., Zwick, F.: Metal foams as compact high performance heat exchangers. Mech. Mater. **35**(12), 1161–1176 (2003)
7. Liu, X.-W., Sun, T.-J., Hu, J.-L., Wang, S.-D.: Composites of metal-organic frameworks and carbon-based materials: preparations, functionalities and applications. Journal of Materials Chemistry A **4**(10), 3584–3616 (2016)
8. Katona, B., Orbulov, I.: Structural damages in syntactic metal foams caused by monotone or cyclic compression. Periodica Polytechnica Mechanical Engineering **61**(2), 146–152 (2017)
9. Maróti, J.E., Orbulov, I.N.: Characteristic compressive properties of AlSi7Mg matrix syntactic foams reinforced by Al2O3 or SiC particles in the matrix. Mater. Sci. Eng., A **869**, 144817 (2023)
10. Gonzalez-Narvaez, R.E., Lopez de Haro, M., Vázquez, F.: Internal structure and heat conduction in rigid solids: a two-temperature approach. J. Non-Equilib. Thermodyn. **47**(1), 13–30 (2022)
11. Sobolev, S.L.: Nonlocal two-temperature model: Application to heat transport in metals irradiated by ultrashort laser pulses. Int. J. Heat Mass Transf. **94**, 138–144 (2016)

12. Both, S., Czél, B., Fülöp, T., Gróf, G., Gyenis, Á., Kovács, R., Ván, P., Verhás, J.: Deviation from the Fourier law in room-temperature heat pulse experiments. J. Non-Equilib. Thermodyn. **41**(1), 41–48 (2016)
13. Sobolev, S.L.: Heat conduction equation for systems with an inhomogeneous internal structure. J. Eng. Phys. Thermophys. **66**(4), 436–440 (1994)
14. Gróf, G.: Notes on using temperature-dependent thermal diffusivity - forgotten rules. J. Therm. Anal. Calorim. **132**, 1389–1397 (2018)
15. McNelly, T.F., Rogers, S.J., Channin, D.J., Rollefson, R.J., Goubau, W.M., Schmidt, G.E., Krumhansl, J.A., Pohl, R.O.: Heat pulses in NaF: onset of second sound. Phys. Rev. Lett. **24**(3), 100–102 (1970)
16. McNelly, T. F.: Second Sound and Anharmonic Processes in Isotopically Pure Alkali-Halides. (1974). Ph.D. Thesis, Cornell University
17. Fehér, A., Kovács, R.: On the dynamic thermal conductivity and diffusivity observed in heat pulse experiments. J. Non-Equilib. Thermodyn. **49**, 161–170 (2024)
18. Fabrizio, M., Lazzari, B., Tibullo, V.: Stability and thermodynamic restrictions for a dual-phase-lag thermal model. Journal of Non-Equilibrium Thermodynamics, (2017). Published Online:2017/01/10
19. Rukolaine, S.A.: Unphysical effects of the dual-phase-lag model of heat conduction: higher-order approximations. Int. J. Therm. Sci. **113**, 83–88 (2017)
20. Kovács, R.: Heat equations beyond Fourier: From heat waves to thermal metamaterials. Phys. Rep. **1048**, 1–75 (2024)
21. Auriault, J.-L.: Cattaneo-Vernotte equation versus Fourier thermoelastic hyperbolic heat equation. Int. J. Eng. Sci. **101**, 45–49 (2016)
22. Jaunich, M., Raje, S., Kim, K., Mitra, K., Guo, Z.: Bio-heat transfer analysis during short pulse laser irradiation of tissues. Int. J. Heat Mass Transf. **51**(23–24), 5511–5521 (2008)
23. Farlow, S. J.: Partial differential equations for scientists and engineers. Courier Corporation, (1993)
24. Gurevich, L.É., Shklovskii, B.I.: Theory of the second sound in semiconductors. Soviet Physics-Solid State **8**, 2434–2438 (1967)
25. Jackson, H.E., Walker, C.T.: Thermal conductivity, second sound and phonon-phonon interactions in NaF. Phys. Rev. B **3**(4), 1428–1439 (1971)
26. Guyer, R.A., Krumhansl, J.A.: Solution of the linearized phonon Boltzmann equation. Phys. Rev. **148**(2), 766–778 (1966)
27. Dreyer, W., Struchtrup, H.: Heat pulse experiments revisited. Continuum Mech. Thermodyn. **5**, 3–50 (1993)
28. Guyer, R.A., Krumhansl, J.A.: Dispersion relation for second sound in solids. Phys. Rev. **133**(5A), A1411 (1964)
29. Ván, P., Berezovski, A., Engelbrecht, J.: Internal variables and dynamic degrees of freedom. J. Non-Equilib. Thermodyn. **33**(3), 235–254 (2008)
30. Berezovski, A., Ván, P.: Internal Variables in Thermoelasticity. Springer, (2017)
31. Landau, L.: Two-fluid model of liquid Helium II. J. Phys. USSR **5**, 71 (1941)
32. Tisza, L.: The theory of liquid Helium. Phys. Rev. **72**(9), 838–877 (1947)
33. Balibar, S.: Laszlo Tisza and the two-fluid model of superfluidity. C R Phys. **18**(9–10), 586–591 (2017)
34. Donnelly, R.J.: The two-fluid theory and second sound in liquid Helium. Phys. Today **62**(10), 34–39 (2009)
35. Schwab, K., Henriksen, E.A., Worlock, J.M., Roukes, M.L.: Measurement of the quantum of thermal conductance. Nature **404**, 974–977 (2000)
36. Müller, I., Ruggeri, T.: Rational Extended Thermodynamics. Springer (1998)
37. Mezhov-Deglin, L.P.: Thermal conductivity of pure lead crystals at low temperatures. Soviet Journal of Experimental and Theoretical Physics **50**, 369 (1979)
38. Rogers, S.J.: Transport of heat and approach to second sound in some isotropically pure alkali-halide crystals. Phys. Rev. B **3**(4), 1440 (1971)
39. Lunev, A., Lauerer, A., Zborovskii, V., Léonard, F.: Digital twin of a laser flash experiment helps to assess the thermal performance of metal foams. Int. J. Therm. Sci. **181**, 107743 (2022)
40. Ván, P., Berezovski, A., Fülöp, T., Gróf, G., Kovács, R., Lovas, Á., Verhás, J.: Guyer-Krumhansl-type heat conduction at room temperature. EPL **118**(5), 50005 (2017). arXiv:1704.00341v1
41. Tzou, D.Y.: A unified field approach for heat conduction from macro- to micro-scales. J. Heat Transfer **117**(1), 8–16 (1995)
42. Matolcsi, T.: Ordinary Thermodynamics. Akadémiai Kiadó (2004)
43. de Groot, S.R., Mazur, P.: Non-Equilibrium Thermodynamics. Dover Publications (1963)
44. Lebon, G., Machrafi, H., Grmela, M., Dubois, C.: An extended thermodynamic model of transient heat conduction at sub-continuum scales. Proceedings of the Royal Society A: Mathematical, Physical and Engineering Sciences **467**(2135), 3241–3256 (2011)
45. Sellitto, A., Cimmelli, V.A., Jou, D.: Mesoscopic Theories of Heat Transport in Nanosystems, vol. 6. Springer (2016)
46. Szücs, M., Munafo, C. F., Kovács, R.: Investigating the whirling heat current density in the Guyer–Krumhansl equation. (2024). arXiv:2405.09199
47. Nyíri, B.: On the entropy current. J. Non-Equilib. Thermodyn. **16**(2), 179–186 (1991)
48. Ván, P.: Weakly nonlocal irreversible thermodynamics - the Guyer-Krumhansl and the Cahn-Hilliard equations. Physic Letters A **290**(1–2), 88–92 (2001)
49. Ván, P., Fülöp, T.: Universality in heat conduction theory - weakly nonlocal thermodynamics. Annalen der Physik (Berlin) **524**(8), 470–478 (2012)
50. Szücs, M., Pavelka, M., Kovács, R., Fülöp, T., Ván, P., Grmela, M.: A case study of non-Fourier heat conduction using Internal Variables and GENERIC. Journal of Non-Equilibrium Thermodynamics, (2021)
51. Rieth, Á., Kovács, R., Fülöp, T.: Implicit numerical schemes for generalized heat conduction equations. Int. J. Heat Mass Transf. **126**, 1177–1182 (2018)
52. Kovács, R., Ván, P.: Generalized heat conduction in heat pulse experiments. Int. J. Heat Mass Transf. **83**, 613–620 (2015)